NASA/TM—2002-211572

Three Dimensional CFD Analysis of the GTX Combustor

C.J. Steffen, Jr.
Glenn Research Center, Cleveland, Ohio

R.B. Bond and J.R. Edwards
North Carolina State University, Raleigh, North Carolina

June 2002

The NASA STI Program Office . . . in Profile

Since its founding, NASA has been dedicated to the advancement of aeronautics and space science. The NASA Scientific and Technical Information (STI) Program Office plays a key part in helping NASA maintain this important role.

The NASA STI Program Office is operated by Langley Research Center, the Lead Center for NASA's scientific and technical information. The NASA STI Program Office provides access to the NASA STI Database, the largest collection of aeronautical and space science STI in the world. The Program Office is also NASA's institutional mechanism for disseminating the results of its research and development activities. These results are published by NASA in the NASA STI Report Series, which includes the following report types:

- TECHNICAL PUBLICATION. Reports of completed research or a major significant phase of research that present the results of NASA programs and include extensive data or theoretical analysis. Includes compilations of significant scientific and technical data and information deemed to be of continuing reference value. NASA's counterpart of peer-reviewed formal professional papers but has less stringent limitations on manuscript length and extent of graphic presentations.

- TECHNICAL MEMORANDUM. Scientific and technical findings that are preliminary or of specialized interest, e.g., quick release reports, working papers, and bibliographies that contain minimal annotation. Does not contain extensive analysis.

- CONTRACTOR REPORT. Scientific and technical findings by NASA-sponsored contractors and grantees.

- CONFERENCE PUBLICATION. Collected papers from scientific and technical conferences, symposia, seminars, or other meetings sponsored or cosponsored by NASA.

- SPECIAL PUBLICATION. Scientific, technical, or historical information from NASA programs, projects, and missions, often concerned with subjects having substantial public interest.

- TECHNICAL TRANSLATION. English-language translations of foreign scientific and technical material pertinent to NASA's mission.

Specialized services that complement the STI Program Office's diverse offerings include creating custom thesauri, building customized data bases, organizing and publishing research results . . . even providing videos.

For more information about the NASA STI Program Office, see the following:

- Access the NASA STI Program Home Page at *http://www.sti.nasa.gov*

- E-mail your question via the Internet to help@sti.nasa.gov

- Fax your question to the NASA Access Help Desk at 301–621–0134

- Telephone the NASA Access Help Desk at 301–621–0390

- Write to:
  NASA Access Help Desk
  NASA Center for AeroSpace Information
  7121 Standard Drive
  Hanover, MD 21076

NASA/TM—2002-211572

Three Dimensional CFD Analysis of the GTX Combustor

C.J. Steffen, Jr.
Glenn Research Center, Cleveland, Ohio

R.B. Bond and J.R. Edwards
North Carolina State University, Raleigh, North Carolina

Prepared for the
Combustion, Airbreathing Propulsion, Propulsion Systems Hazards,
and Modelling and Simulation Subcommittees Joint Meeting
sponsored by the Joint Army-Navy-NASA-Air Force
Destin, Florida, April 8–12, 2002

National Aeronautics and
Space Administration

Glenn Research Center

June 2002

Acknowledgments

The subsonic combustion analysis has been funded under an NRA grant from NASA Glenn Research Center under the Base Research and Technology Programs Office: grant number NAG3–2658. The authors would like to express their appreciation to Dr. Hani Kamawi for help with interpreting the direct-connect test results.

This report contains preliminary findings, subject to revision as analysis proceeds.

The Aerospace Propulsion and Power Program at NASA Glenn Research Center sponsored this work.

Available from

NASA Center for Aerospace Information
7121 Standard Drive
Hanover, MD 21076

National Technical Information Service
5285 Port Royal Road
Springfield, VA 22100

Available electronically at http://gltrs.grc.nasa.gov/GLTRS

THREE DIMENSIONAL CFD ANALYSIS OF THE GTX COMBUSTOR

C. J. Steffen, Jr.[†]
National Aeronautics and Space Administration
Glenn Research Center
Cleveland, Ohio 44135

R.B. Bond[‡] and J. R. Edwards[ł]
North Carolina State University
Raleigh, North Carolina 27695-7910

ABSTRACT

The annular combustor geometry of a combined-cycle engine has been analyzed with three-dimensional computational fluid dynamics. Both subsonic combustion and supersonic combustion flowfields have been simulated. The subsonic combustion analysis was executed in conjunction with a direct-connect test rig. Two cold-flow and one hot-flow results are presented. The simulations compare favorably with the test data for the two cold flow calculations; the hot-flow data was not yet available. The hot-flow simulation indicates that the conventional ejector-ramjet cycle would not provide adequate mixing at the conditions tested. The supersonic combustion ramjet flowfield was simulated with frozen chemistry model. A five-parameter test matrix was specified, according to statistical design-of-experiments theory. Twenty-seven separate simulations were used to assemble surrogate models for combustor mixing efficiency and total pressure recovery. Scramjet injector design parameters (injector angle, location, and fuel split) as well as mission variables (total fuel massflow and freestream Mach number) were included in the analysis. A promising injector design has been identified that provides good mixing characteristics with low total pressure losses. The surrogate models can be used to develop performance maps of different injector designs. Several complex three-way variable interactions appear within the dataset that are not adequately resolved with the current statistical analysis.

INTRODUCTION

NASA is presently studying several advanced propulsion systems that promise to provide affordable access to space. One concept, the reusable SSTO "GTX", is based upon Rocket Based Combined Cycle (RBCC) propulsion. A three-view schematic is shown below in Figure 1, along with the engine flowpath. An axisymmetric engine design has been created. Structural and analytical simplicity are the direct result.

The operational scenario for GTX consists of four modes of propulsion. In the first mode, valid from liftoff to about Mach 2.5, the engine operates in a so-called independent ramjet stream (IRS) cycle, where rocket thrust is initially used for primary power and as an ignition source for hydrogen fuel injected directly into the inlet air. Ignition and combustion of this fuel source, as well as unburned rocket fuel, results in the formation of a thermal throat in the nozzle and a ramjet mode of operation for the secondary stream. As the Mach number increases, the percentage of thrust due to the ramjet alone increases, and around Mach 2.5, the rocket motor is shut off and the engine shifts to a pure ramjet mode of operation (second mode). Around Mach 6, it becomes more practical to burn at supersonic speeds, and aided by centerbody translation, the engine shifts to a scramjet mode (third mode). The rocket is re-ignited around Mach 11 (fourth mode), the centerbody is translated to shut the inlet flow completely off, and the engine shifts to a rocket-only propulsion mode for the remainder of the ascent. Further details on the operation of this propulsion cycle are available in reference[1].

The air-breathing combustor operates during the first three modes, and a conventional rocket combustor operates during the first and fourth mode. The air-breathing combustion process can be further segregated into subsonic (mode 1&2) and supersonic (mode 3) regimes. The single flowpath concept presents a design challenge for the air-breathing combustor. Location of the fuel injection ports must optimize the performance of the entire air-

[†] Aerospace engineer, Engine Systems Technology Branch, c.j.steffen@grc.nasa.gov
[‡] Graduate Research Assistant, Department of Aerospace and Mechanical Engineering, rbbond@eos.ncsu.edu
[ł] Associate Professor, Department of Aerospace and Mechanical Engineering, jredward@eos.ncsu.edu

breathing portion of the trajectory. CFD offers an efficient analysis method, when coupled with ongoing experimental efforts, to estimate combustor efficiencies and generate 3D design-specific fluids analysis.

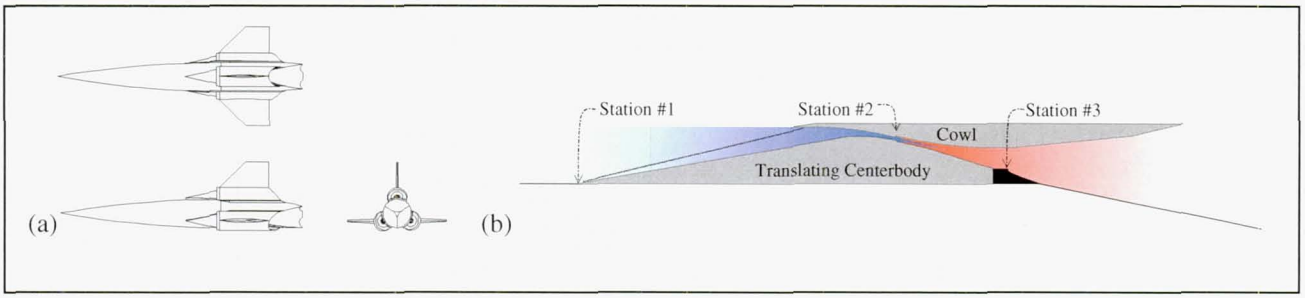

Figure 1 (a) Three view schematic drawing of the GTX reference vehicle, and (b) axisymmetric flowpath geometry.

BACKGROUND

Initial Navier-Stokes analysis of the air-breathing combustor was conducted to demonstrate baseline performance[2]. Both subsonic (2D) and supersonic (3D) combustion analyses were presented. The investigation of subsonic combustion examined the influence of fuel-air ratio, fuel distribution, and rocket chamber pressure upon the combustion physics and thermal choke characteristics. Results indicated that adjustment of the amount and radial distribution of fuel can control the thermal choke point. The secondary massflow rate was very sensitive to the fuel-air ratio and the rocket chamber pressure. The investigation of supersonic combustion examined the influence of fuel-air ratio and fuel injection schedule upon combustion performance estimates. An analysis of the mesh-dependence of these calculations was presented. Jet penetration data was extracted from the three-dimensional simulations and compared favorably with experimental correlations of similar flows. Results indicated that combustion efficiency was very sensitive to the fuel schedule.

A simplified fuel injection strategy was employed for the initial (2D) IRS. Three-dimensional analysis of the low-speed combustion process can increase the fidelity of analysis by addressing the effects of discrete fuel injection, combustor enwalls, and 3D ducted rocket effects. Additionally, the dynamic effects of mode transition during the low-speed regime are of interest as well. A research effort to address these issues has been initiated.

The initial (3D) scramjet analysis was limited to a small range of parametric variation of the fuel injection strategy. Good combustion efficiency was achievable with a normal injection scheme, at the cost of creating a strong reflected shock system. Several interacting effects precluded any concise analysis. A systematic effort to optimize the fuel injection strategy within this flowpath was initiated. The present work is divided into two sections according to the separate analysis efforts. The numerical models and results applicable to subsonic combustion analysis are presented together in one section. A separate presentation of the methods and results applicable to supersonic combustion analysis follows. Together, this work represents a snapshot of the progress to date of the 3D combustion analysis within the GTX program.

SUBSONIC COMBUSTION ANALYSIS

MODE 1: EJECTOR-RAMJET (IRS CYCLE)

The Independent Ramjet Stream (IRS) cycle, a variation of the conventional ejector-ramjet, is currently being evaluated for use as the low speed propulsion mode of GTX[3]. In a conventional ejector-ramjet, a fuel-rich rocket exhaust is mixed and burned with air captured by the inlet. The rocket provides all of the fuel needed for combustion with the entrained air. The main disadvantage of this concept is the relatively long duct required to achieve complete mixing of the air and rocket streams. In the IRS cycle, the airstream is fueled independently using the ramjet and scramjet mode fuel injectors located in the inlet diffuser, as shown in Figure 2. The rocket serves as a pilot for the fueled airstream.

The goal of this Mode 1 study is to conduct a CFD investigation of the IRS cycle on the geometry currently being tested at GRC[4]. The objectives are to understand the flow and combustion physics of engine operation during Mode 1 operation and the transition to Mode 2. The initial efforts are directed towards simulating steady-state performance of the geometry during cold-flow operation and conventional ejector-ramjet operation. Computational results will be compared with test data, where available.

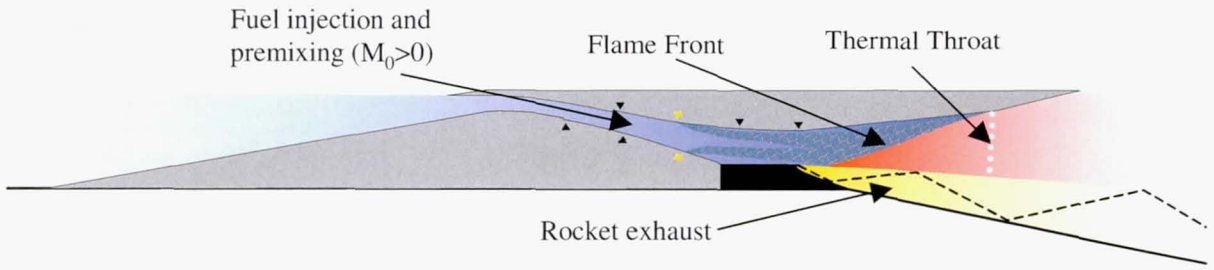

Figure 2 Schematic drawing of the IRS propulsion mode.

NUMERICAL METHODS

The computational analysis is based upon a validated Navier-Stokes solver for unsteady reactive-flow calculations on massively parallel machines[5,6,7]. The current approach combines high-resolution upwind differencing strategies[8,9] with a dual-time stepping (or sub iteration) procedure for recovering second order temporal accuracy. A key feature of the approach is the use of highly implicit incomplete block factorization or planar Gauss-Seidel methods to alleviate stability restrictions due to severe grid stretching. This allows the use of physical time steps much larger than the inviscid stability limit, a feature that is particularly important as flowpath responses may be very slow, compared to typical characteristic time scales. Computational efficiency is maintained by storing the factorization of system Jacobian matrix in core memory for the particular block (or group of blocks) mapped to a particular processor. After initial transients have been purged, the factorization only needs to be re-evaluated every few iterations, significantly reducing the overall expense. Parallelization of the solver is accomplished through standard domain-decomposition strategies, with communication between processors facilitated by MPI routines. Balakrishnan's 9 species / 24 reaction mechanism[10] is currently used to model hydrogen oxidation. Turbulent effects are handled by Menter's hybrid k-ε / k-ω two-equation turbulence model.

The solver has been validated through steady-state simulations of the 3-D shock / hydrogen flame experiments of Driscoll and co-workers[5], among other cases. Dynamic simulations of the response of a complete scramjet inlet-combustor configuration to time-dependent hydrogen fuel injection have also been conducted in two and three dimensions[6,7].

GEOMETRY AND TEST CONDITIONS

Case	$\dot{m}_{air}$ (lbm/s)	T_o (R)	P_b (psia)	Rocket Chamber Pressure (psia)	Rocket Exit Pressure (psia)	IRS fuel $\dot{m}_{sf}$ (lbm/s)	Rocket Chamber Temp. (R)	Rocket Mixture Ratio
1. ESP#41 (cold flow)	9.94	547	8.2	N/A	N/A	N/A	N/A	N/A
2. ESP#39 (cold flow)	9.94	547	3.1	N/A	N/A	N/A	N/A	N/A
3. Mach 2.5 (ejector ramjet)	22.0	877	N/A	500	8.3	N/A	7063	6

Table 1 Mode 1 simulation conditions.

The GTX geometry currently being tested at NASA GRC's direct-connect facility consists of a translating centerbody mounted on a flat plate within a surrounding contoured cowl section, semicircular in cross-section. The geometry is scaled to cowl lip radius of 11 inches. The forward section of the contoured centerbody, also semicircular in cross-section, mimics the internal area-ratio profile of the actual engine. A backward-facing step behind the centerbody maximum area point provides inlet isolation. A combustor section (50 inches long) is attached to the centerbody section. The outer (cowl side) part of the combustor section diverges at a constant angle of 5 degrees. A rocket motor is located within the centerbody. During operation, the rocket plume exhausts parallel to the flat plate. Fuel injection locations are provided at different axial intervals upstream and downstream of the centerbody /combustor juncture. Two fuel injector banks are located upstream of the centerbody / combustor juncture. Each bank consists of 11 fuel injectors (0.2 inches in diameter), equally spaced around the semicircular cowl surface. These pilot the ramjet air-stream during Mode 1 IRS cycle operation. Other fuel injector banks are located within the combustor. During operation as a conventional ejector-ramjet, all fuel injector banks are shut off, and only excess hydrogen within the rocket exhaust fuels the primary air stream. Further details regarding the test

geometry are given elsewhere[4]. Results presented herein correspond to simulations conducted at two cold-flow conditions and one ejector-ramjet condition. Pertinent parameters are shown in Table 1. These comprise portions of the cold-flow / hot-flow GTX test matrix. The symbol ($\dot{m}_{sf}$) represents the mass flow rate of secondary fuel injection upstream of the centerbody / combustor juncture.

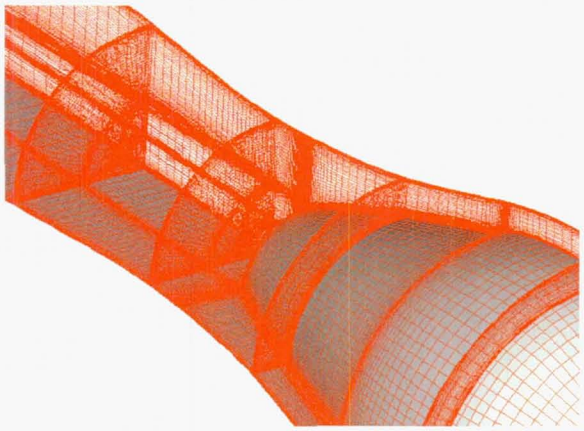

Figure 3 Grid for ejector-ramjet simulations: flow is in the positive (x) direction

A typical computational grid used in the GTX simulations is shown in Figure 3. Half-plane symmetry with respect to the Y-axis is assumed. This particular grid corresponds to that used for the ejector-ramjet simulations and contains roughly 2.27 million cells. The grid used for the cold-flow simulations also contains approximately 2.27 million cells but is simpler in topology, as no attempt is made to resolve the rocket exit plane geometry. A patched-grid boundary condition connects this section of the geometry to the combustor section, which is rendered exactly as used in the ejector-ramjet calculations. The domain is divided into discrete load-balanced blocks for mapping onto 98 processors of an IBM SP-2 server at the North Carolina Supercomputing Center.

COLD FLOW RESULTS

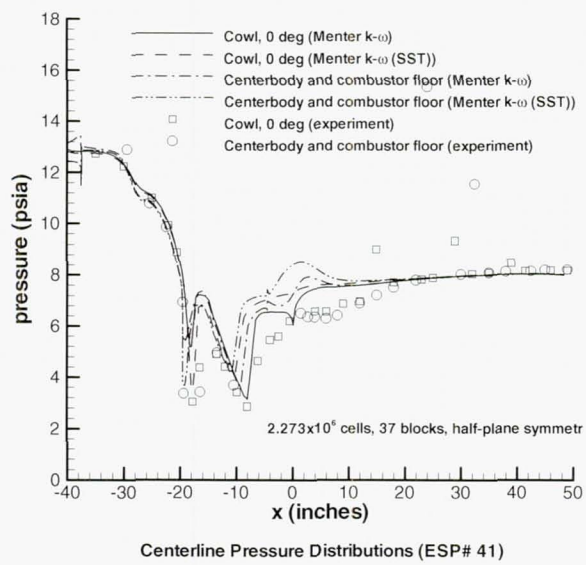

Figure 4 Centerline pressure profile

Simulations without rocket or secondary fuel injection were conducted at conditions corresponding to cases 1 and 2 above. Figure 4 and Figure 5 present pressure distributions along the centerbody / flat plate surface and along the cowl surface at the Y = 0 plane. The scale of the X-axis is referenced to station #3. Both cases resulted in a transition to supersonic flow at the minimum area location (station #2), followed by a compression and expansion region resulting from the changing flowpath area profile. At this point (approximately x=-10in) the two solutions will differ due to the backpressure ratio applied. Case 1 (ESP #41) resulted in a shock-induced separation, upstream of station #3, and subsonic flow at the exit. Case 2 (ESP #39) continued to expand supersonically beyond station #3, and experienced a shock-induced separation downstream along the flatplate surface. This resulted in a mixed subsonic/supersonic flow at the combustor exit.

Figure 4 also compares results from two turbulence models: Menter's baseline model and Menter's model with the SST (shear-stress transport) modification. The SST modification tends to reduce the production of eddy viscosity in adverse pressure gradient flows and generally will result in larger separation regions than provided by the baseline model. Figure 4 shows that this trend was somewhat detrimental, as the position of the terminating normal shock (X ~ -9 in) was better predicted by the baseline model, which resulted in less axial separation in the combustor section.

The expansion of the flow into the combustor and the location of the recompression was predicted well by the model, as shown in Figure 5. However, as in case 1, the initial expansion of the flow behind the backward-facing step was underpredicted. It is likely that the structure of the flow in this region was influenced by whether it is laminar or turbulent. The turbulent flow prediction, illustrated in Figure 5, tended to result in a thicker boundary

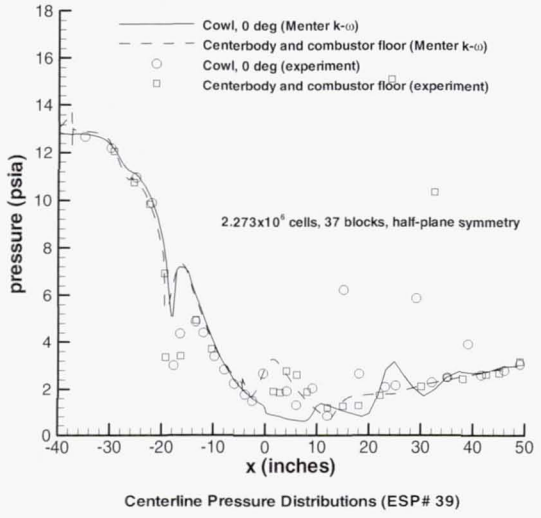

Figure 5 Centerline pressure profile

layer upstream of the step and a more elongated region of axially separated flow. The associated displacement effects would tend to smooth out the rapid expansion more than if the flow was modeled as laminar or transitional in this region.

EJECTOR-RAMJET RESULTS

In a conventional ejector-ramjet, the rocket is operated at fuel-rich conditions. Excess fuel within the hot rocket exhaust then mixes with primary air and ignites, resulting in combustion within the primary air stream. The GTX hot-flow test matrix includes several ejector-ramjet cases, but as of this writing, no experimental data has been released. Conditions for the particular case considered herein correspond to flight at Mach 2.5, just prior to the shift to full ramjet mode at about Mach 3. Backpressure ranges for the hot-flow tests are not yet available; the simulation described next assumes a fully supersonic flow at the combustor exit. Figure 6 presents hydroxyl (OH) mass fractions and temperature contours for this case. The maximum OH contour marked the flame front, which extended outward from the rocket exit plane as the rocket exhaust mixed with the primary air stream.

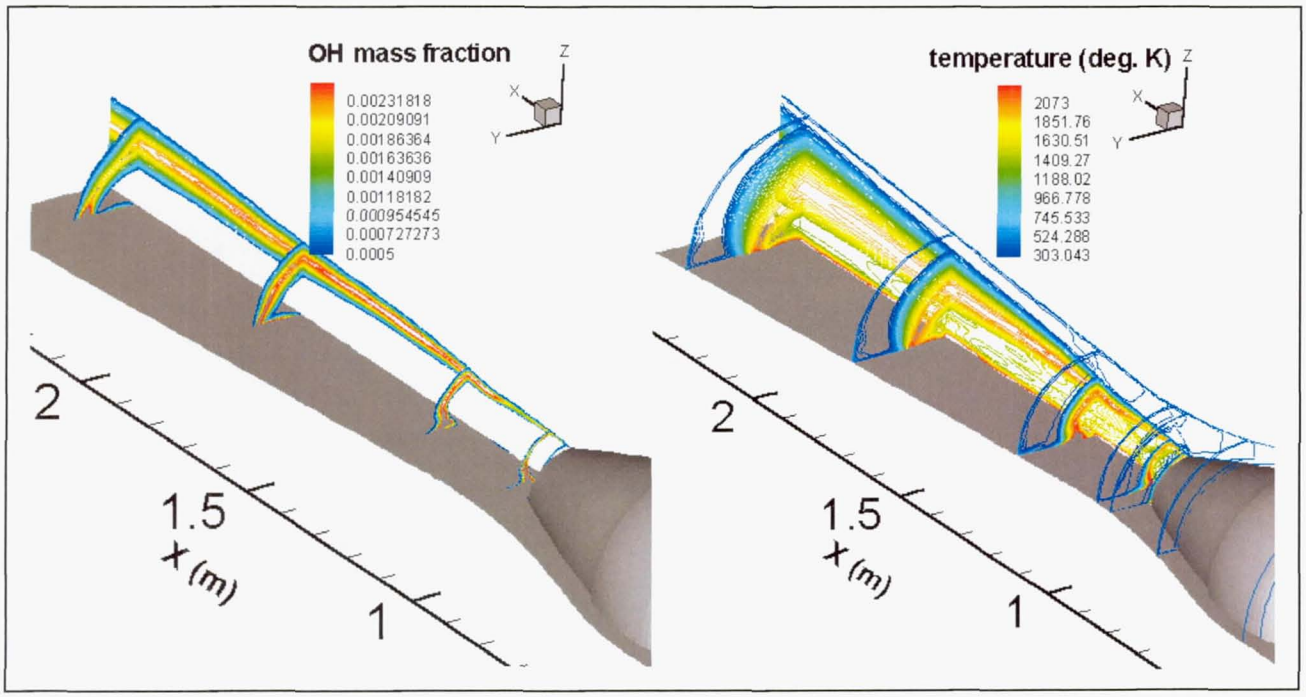

Figure 6 OH and temperature contours for a Mach 2.5 ejector-ramjet configuration

Temperatures of around 2000K degrees are found in the vicinity of the flame front, though hotter (~3200 K) temperatures are obtained where the rocket impinges upon the flat plate. The amount of heat release provided at this condition ($\Phi = 0.08$) is not enough to overcome the tendency of the entering supersonic flow to accelerate in a divergent duct, and the average Mach number of the air stream at the combustor exit is around 2.2. As the rocket exhaust itself enters the combustor at around 1850 K, the flame ignites almost immediately and is stabilized just behind the rocket exit plane. Figure 6 shows that the mixing layer does not encompass the inlet air stream before exiting the 50inch combustor, thus complete mixing was not going to be possible at this equivalence ratio (ϕ=0.08).

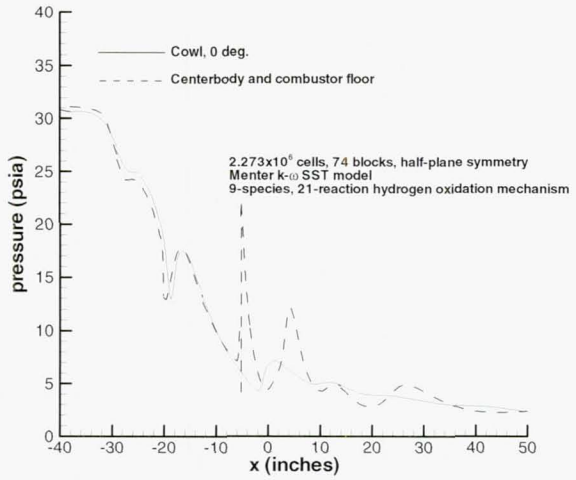

Figure 7 Centerline pressure profile: Mach 2.5 ejector-ramjet

Figure 7 presents pressure distributions along the cowl, centerbody, and combustor floor centerlines. The oblique shock system formed as the rocket exhaust impinges on the combustor floor is clearly indicated. After an initial rise due to the impingement of an oblique shock resulting from the rocket displacement into the outer stream, the combustor cowl pressure levels decrease.

The IRS cycle should enable more rapid mixing by injecting the fuel upstream of station #3. Two-dimensional analysis of this process has been encouraging; current efforts are directed at three-dimensional analysis of this new propulsion cycle.

SUPERSONIC COMBUSTION

MODE 3: SCRAMJET CYCLE

Our combustion efficiency target for the scramjet cycle operation has been fixed at 92.5%. The concept behind the current scramjet combustor design includes two different fuel injection locations located between stations #2 and #3, as shown in Figure 8. The first set of injectors were placed at station #2 and constituted the "streamwise" injection ports, located in the backstep region of both the cowl and centerbody. These streamwise injectors fueled the flame holding region of the combustor and perhaps, supplied a substantial portion of the required fuel. The second set of fuel injectors, flush-wall "transverse" injection ports, was placed in the constant area portion (first 25%) of the scram combustor flowpath. The transverse injectors were located in opposing fashion, along both the cowl and centerbody walls at a given station (either fwd, mid or aft station).

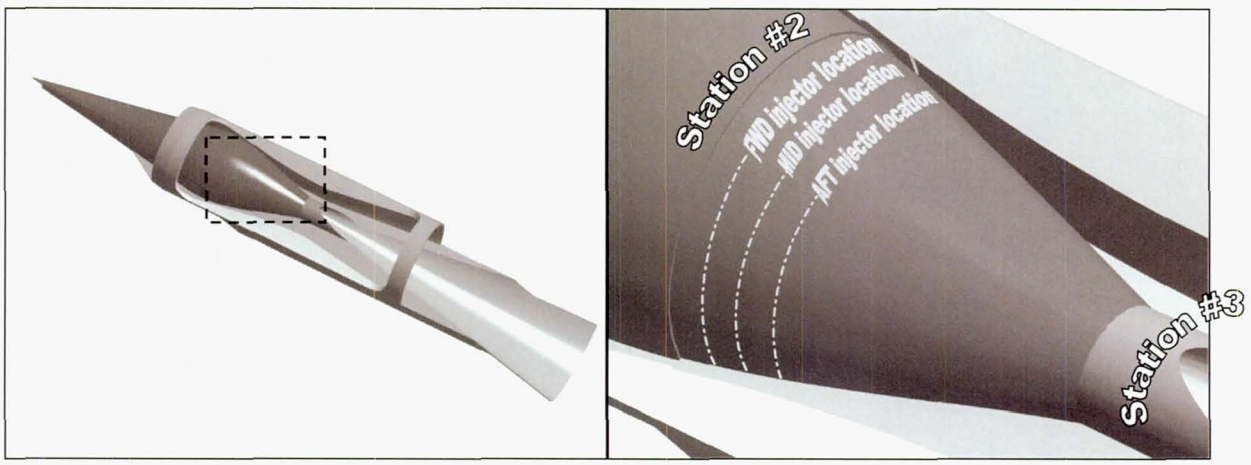

Figure 8 Propulsion assembly cutaway drawing and close-up view of the scramjet combustor region

As mentioned earlier, initial scramjet combustion simulations were able to demonstrate good mixing results at the expense of strong shock systems and a substantial blockage effect within the constant area section of the scram combustor. This resulted in a total pressure loss, and a drop in the core flow Mach number to near-sonic or subsonic levels. Several possibilities exist to remedy this situation, based upon answers to the following questions:

1. How important are transverse injector angle and location?
2. How important is axial injection in the backstep region, beyond flameholding?
3. How should a given amount of fuel be distributed between the transverse and axial injectors?

4. How much benefit is derived from running the engine in a fuel-rich mode?
5. How do these parameters interact with increasing freestream Mach number?

	Lower limit	Mid-range	Higher limit
(x_1) **Fuel split** (step inj.(%)--wall inj.(%))	25%---75%	50%---50%	75%---25%
(x_2) **Wall injector angle** (measured from wall)	15°	45°	75°
(x_3) **Wall injector location** (measured from station #3)	Fwd position -115in	Mid position -102.5in	Aft position –90in
(x_4) **Freestream Mach** (M_0)	6.5	9.25	12
(x_5) **Total equivalence ratio** (ϕ)	1.0 (stoich.)	1.2	1.4

Table 2 Design space for scramjet mixing analysis and optimization

Addressing these questions can lead us towards an injection scheme that achieves the target efficiency required for scramjet operation. One approach to injector performance optimization, based upon a statistical experiment design (DoE), can quantitatively answer the issues raised above. This approach has been applied elsewhere within the aero-propulsion community for system design and engineering problems[11]. A properly executed DOE study would yield a set of surrogate models that characterize the relevant physics from CFD analysis. These polynomial surrogate models can then be exploited for system optimization and/or performance maps. Thus a 27-case ½-fractional central-composite-design (½-CCD) has been used to study the GTX scramjet combustor performance with CFD. The design space was defined as shown in Table 2.

HYPERSONIC FLOW SIMULATIONS

Several important assumptions have been made with regard to scramjet flow simulation. The GTX combustor geometry was designed as a 220° annular section, with planar endwalls. The scramjet CFD simulations neglect the endwall effect and assumed a fully axisymmetric geometry. This simplification enabled the computational domain to be limited by the fuel injector symmetry requirement.

The circumferential distribution (pitch) of fuel injectors was assumed to be of secondary importance to the design optimization. Thus, the circumferential distribution of injectors was fixed at three-degrees for the axial injectors and six-degrees for the transverse injectors. Six-degree-pitch in the constant area combustor corresponded to the transverse gap measurement; this pitch was specified to coincide with the NASA Langley design approach[12]. This assumption will be revisited at the conclusion of this study.

The scramjet flowfield was assumed to be mixing limited, and thus the simulations have been executed with frozen chemistry. An additional calculation was conducted to examine the impact of combustion modeling upon the mixing efficiency. Although this finite-rate-reaction simulation cannot address the turbulent-chemical interaction, it quantified the impact of the mixing-limited assumption upon the present analytical work. The mixing efficiency of the finite-rate-chemistry calculation was approximately 1.5% higher than the frozen chemistry simulation of the design centerpoint (Case #14).

The combustor entrance conditions were specified from decoupled axisymmetric inlet simulations, according to the freestream conditions along a prescribed trajectory[13]. The mixing limited flowfield was modeled with a relatively new turbulence model: Wilcox's 1998 version of the two-equation k-w model[14]. Although no turbulence model has been universally accepted and validated for the challenging environment of a scramjet combustor, this particular model has been shown to perform admirably for free shear flows. Boundary condition values for the turbulent variables were also specified from the axisymmetric inlet flowfield.

The 27 different simulations were executed on one of nine different grids, according to the different transverse injector geometries proscribed in the run matrix, Table 3. The injectors have been specified as choked, sonic conditions for all cases. This demanded that the size of the injection port must vary according to the specified fuel-flow rate, in order to avoid either a subsonic condition at the low end, or a dramatically under-expanded condition at the high end. This variation was accomplished by a grid-generation approach that nested a small port within a larger port. The gaseous hydrogen fuel was injected with a static temperature that varied with freestream Mach number. The fuel temperatures were specified as (1500°R, 2000°R, 2500°R) at Mach (6.5, 9.25, 12) respectively.

The performance analysis was based upon a response surface model, built from 27 different CFD calculations. The experimental design allowed for the linear effects, quadratic effects and two-way interactions of all five parameters; all other higher order effects and interactions were assumed to be negligible. The performance variation across the injector designs was assumed to be much larger than any acknowledged CFD errors, especially

the mesh dependence. This assumption was based upon prior analysis: (1) a mesh-dependent error of approximately 5% could be expected from a (coarse/fine) grid sequence of (280k /2.24M) cells, and (2) mixing efficiency results could be expected to vary by 40% or more based upon the fuel injection scheme. Three fine-mesh simulations have been completed, and the mixing efficiency mesh dependencies were found to be (4.6%, 2.4%, –2.45%). The differences observed across design space varied by approximately sixty percent, as observed in Table 3.

The Navier-Stokes solver used for these solutions was the GASPv4 code. GASP is a 3D, finite volume, structured-mesh RANS solver that has been used to analyze many high-speed propulsion flows, including scramjet combustors, in steady state or time-dependent fashion. A detailed discussion of the numerical methods have been presented elsewhere[15]. Note that the geometry was modeled at the reference vehicle scale, as opposed to the model scale used elsewhere. All results have been converged so that massflux was constant to within $(\pm 1\%)$.

Case #	Step Injector %	Wall Injection Angle (deg)	Wall Injection placement	Mach #	Fuel/Air ratio ϕ_{total}	η_{mix} (%)	P_{03}/P_{02} (%)
1	25%	15	fwd	6.5	1.4	94.1	35.2
2	75%	75	fwd	6.5	1.4	63.9	32.9
3	25%	75	fwd	6.5	1	76.0	34.7
4	75%	15	fwd	6.5	1	41.2	39.3
5	50%	45	mid	6.5	1.2	75.7	33.8
6	75%	15	aft	6.5	1.4	41.3	33.7
7	75%	75	aft	6.5	1	44.3	36.6
8	25%	15	aft	6.5	1	61.3	36.4
9	25%	75	aft	6.5	1.4	91.7	26.6
10	50%	45	mid	9.25	1	61.3	27.1
11	50%	45	mid	9.25	1.4	74.1	22.7
12	25%	45	mid	9.25	1.2	84.5	22.0
13	75%	45	mid	9.25	1.2	43.2	26.6
14	50%	45	mid	9.25	1.2	67.5	24.6
15	50%	75	mid	9.25	1.2	71.0	23.4
16	50%	45	aft	9.25	1.2	47.3	24.8
17	50%	45	fwd	9.25	1.2	51.6	25.9
18	50%	15	mid	9.25	1.2	54.5	27.9
19	25%	15	fwd	12	1	67.2	29.9
20	75%	75	fwd	12	1	51.5	29.5
21	25%	75	fwd	12	1.4	86.8	19.8
22	75%	15	fwd	12	1.4	55.3	26.5
23	50%	45	mid	12	1.2	62.8	24.5
24	75%	15	aft	12	1	34.7	31.1
25	75%	75	aft	12	1.4	44.1	23.9
26	25%	15	aft	12	1.4	52.6	23.4
27	25%	75	aft	12	1	47.5	22.1

Table 3 Design of experiments test matrix for scramjet analysis and optimization

SCRAMJET INJECTOR PERFORMANCE OPTIMIZATION

The construction and execution of this designed experiment was recently discussed[15], however the regression results are presented below for the first time. The objective was to search a broad design space for regions of high performance. This was defined as good mixing efficiency at relatively low total pressure losses. Table 3 shows the mixing efficiency and total pressure loss data from the 27 CFD runs that were used to construct the response models for performance optimization.

A statistical analysis of the above data was performed using the software Design Expert™. Surrogate models have been developed for the mixing efficiency at station #3 $\left(\eta_{mix}\right)$ and the total pressure recovery at station #3 $\left(P_{03}/P_{02}\right)$ and given below. Note that a natural logarithm transformation of the mixing efficiency data $\left(\eta_{mix}^{trans}\right)$ was performed prior to modeling; the mixing efficiency model is back-transformed via the exponential (EXP) function.

$$\left(\eta_{mix}^{trans}\right) = -35.06 - 0.006921\,x_1 + 0.006100\,x_2 - 0.6659\,x_3 - 0.003123\,(x_3)^2 - 0.8379\,x_4 + 0.003589\,x_1\,x_4 + 0.048129\,(x_4)^2 + 6.715\,x_5 - 0.04472\,x_1\,x_5 - 0.2778\,x_4\,x_5$$

$$\left(\eta_{mix}\right)\% = 100.0\,\frac{EXP\left(\eta_{mix}^{trans}\right)}{1+EXP\left(\eta_{mix}^{trans}\right)}$$

Equation 1

A proper interpretation of this polynomial model of mixing efficiency must include the statistical uncertainty $E_{95\%C.I.}^{trans}$. The 95% confidence interval on future prediction of the response is defined below. Note that the uncertainty estimate is based upon Student's t-distribution ($t_{student}$) and the standard error of regression ($S_{trans(y)\bullet x}$) for the transformed data[16].

$$E_{95\%C.I.}^{trans} \approx \pm t_{student}\,S_{logit(y)\bullet x}\;;\; t_{student} = 2.12\;;\; S_{trans(y)\bullet x} = 0.30$$

$$\left(\eta_{mix}^{95\%C.I.}\right)\% \approx 100.0\,\frac{EXP\left(\eta_{mix}^{trans} \pm E_{95\%C.I.}^{trans}\right)}{1+EXP\left(\eta_{mix}^{trans} \pm E_{95\%C.I.}^{trans}\right)}$$

Equation 2

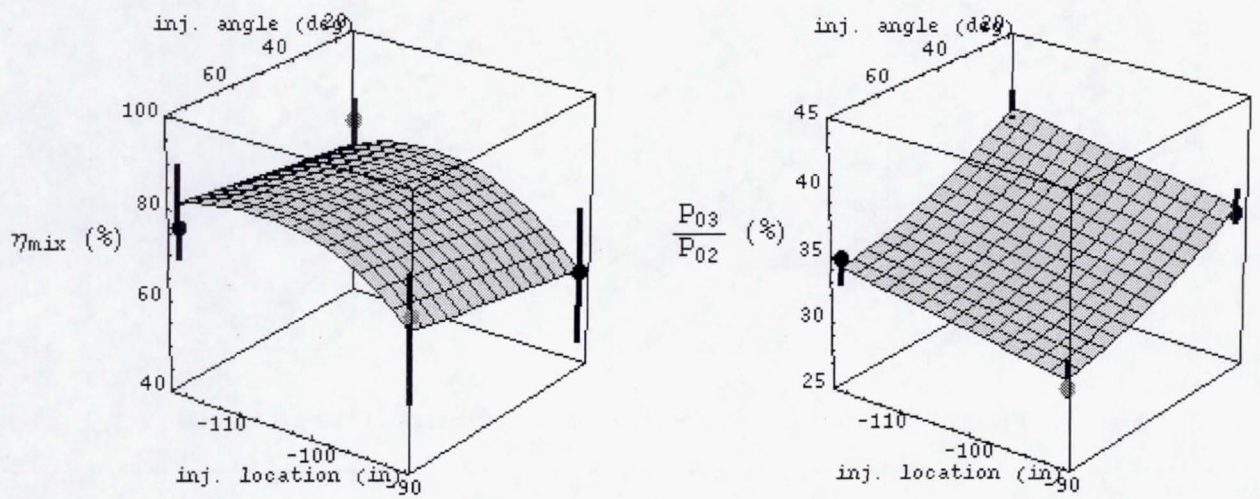

Figure 9 Response surfaces of the mixing efficiency and total pressure recovery as a function of transverse injector geometry (injection angle and location) at M_0=6.5, ϕ_{total}=1 with 25% injected at step: surrogate models are represented as the gray surfaces, the associated 95% confidence intervals are indicated by the vertical lines, test data from Table 1 shown as black dots, and confirmation data shown as gray dots.

The total pressure recovery data was modeled directly, as shown below:

$$\left(P_{03}/P_{02}\right)\% = 94.34 + 0.1326\,x_1 - 0.2138\,x_2 + 0.001181\,x_1\,x_2 + 0.001022\,(x_2)^2 - 0.1508\,x_3 + 0.001675\,x_1\,x_3 - 12.59\,x_4 + 0.005744\,x_1\,x_4 + 0.5789\,(x_4)^2 - 11.60\,x_5$$

$$E_{95\%C.I.}\% \approx \pm t_{student}\; S_{(y)\bullet x}\;;\; t_{student} = 2.12\;;\; S_{(y)\bullet x} = 0.52$$

$$\left(P_{03}/P_{02}\right)^{95\%C.I.}\% \approx \left(P_{03}/P_{02}\right) \pm E_{95\%C.I.}$$

Equation 3

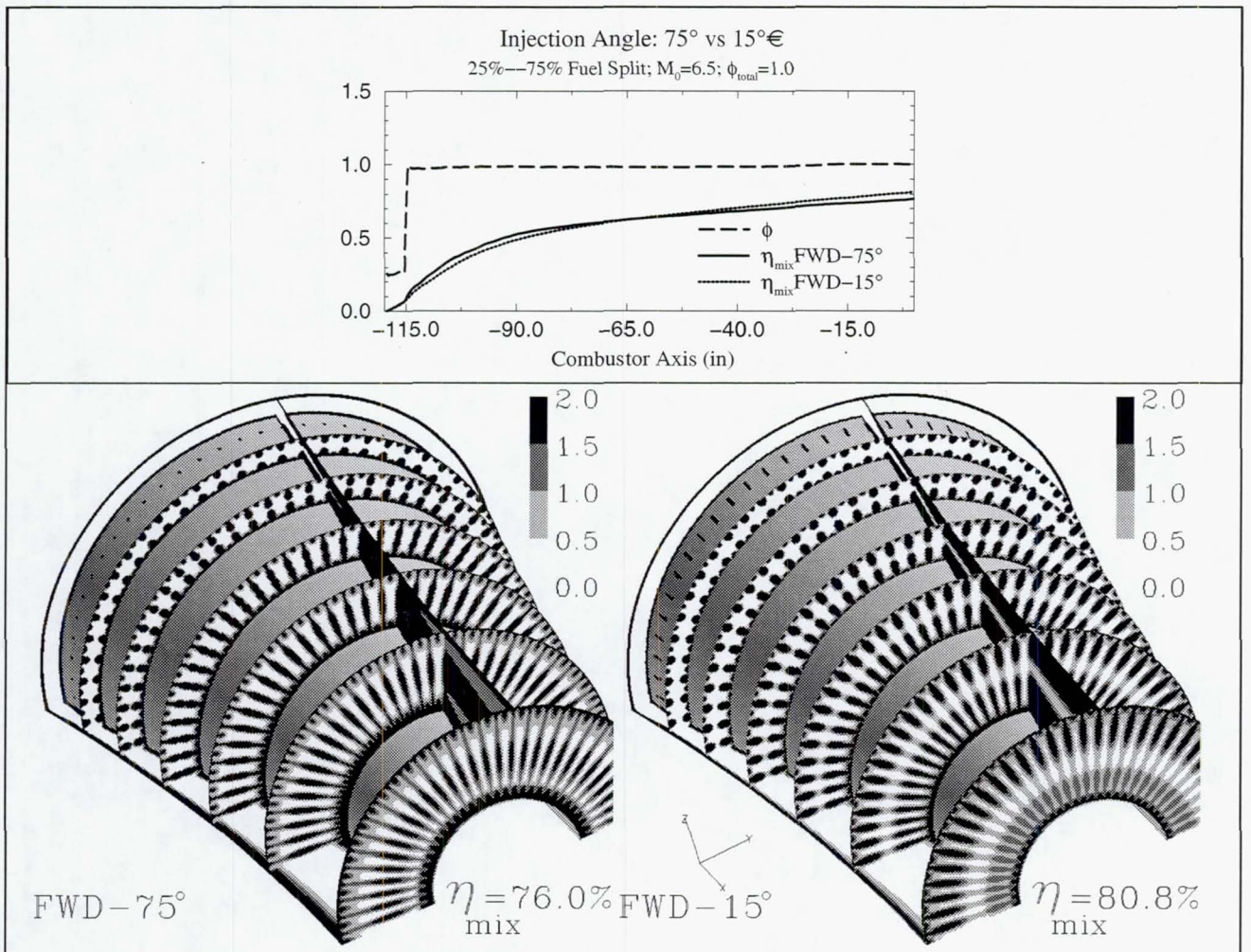

Figure 10 Effect of transverse injection angle on mixing efficiency at Mach 6.5, ϕ=1.0

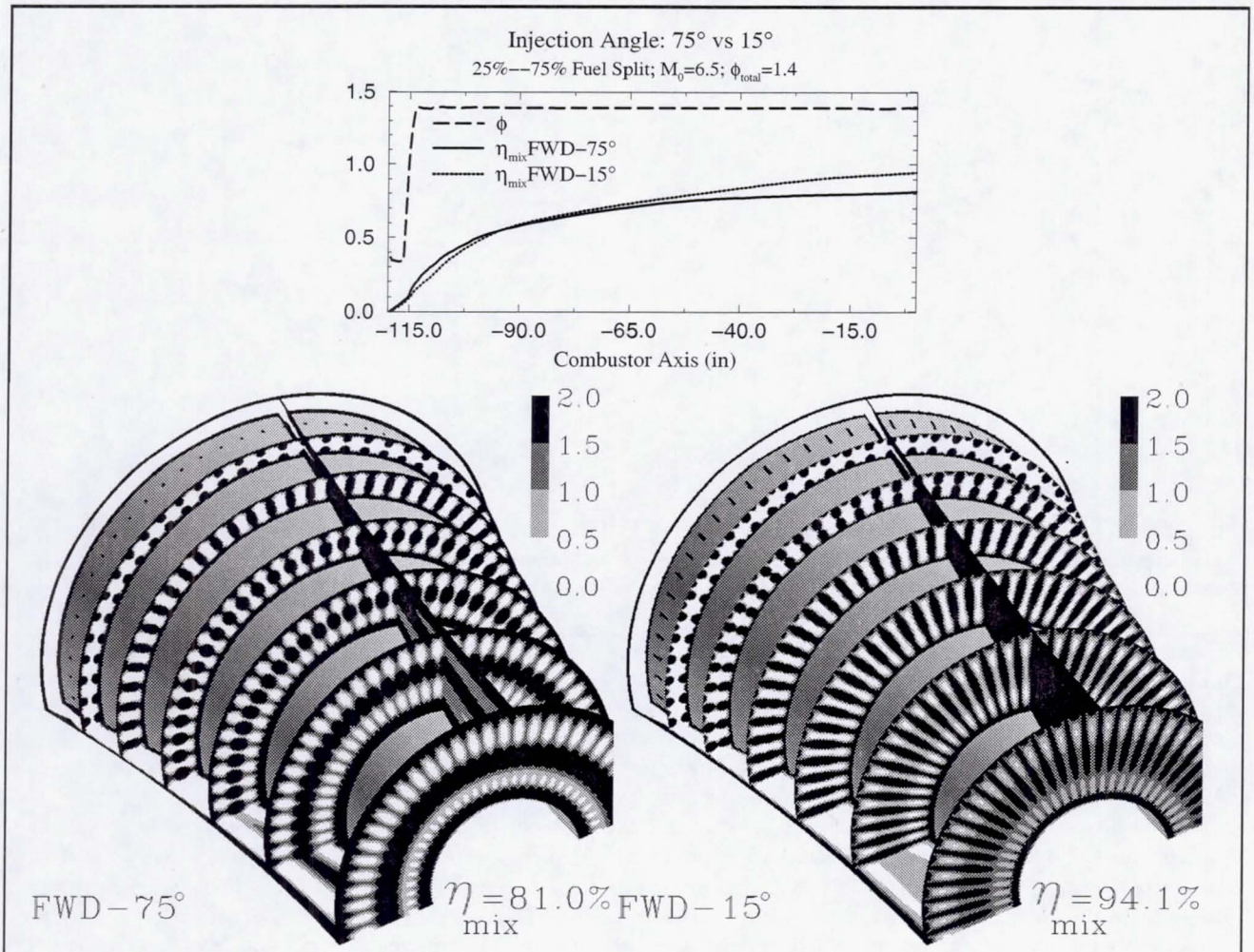

Figure 11 Effect of transverse injection angle on mixing efficiency at Mach 6.5, ϕ=1.4.

Several key features can be observed from the initial RSM analysis. The percentage of fuel injected at the step should be minimized and the total equivalence ratio should be maximized to achieve the highest efficiencies within this design space. The RSM results also implied that a relatively large number of transverse injector designs (angle and location) could be used to achieve good mixing across the Mach number range. This means that relatively low injection angles (fifteen degrees) can be utilized without a significant drop in mixing efficiency. This finding echoed earlier results alluded to in the open literature[17]. The introduction of a second response model for total pressure recovery has enabled further refinement of the design for both good mixing and high total pressure recovery within the combustor. Figure 9 shows the two RSM predictions as a function of injector angle and location. The forward-positioned, low-angle injector (FWD-15°) appeared to have a distinct advantage, when both performance measures are combined.

One must remember that the predictive capability of these results is defined by the polynomial results and the associated uncertainty. Several extra CFD simulation runs have been executed to explore the efficacy of this model for further optimization. Consider the data presented in Figure 9: the model predicted a small decrement in mixing performance when the injector angle is reduced from 75° towards 15°. However, additional CFD results imply that a significant interaction between the injector angle and location exists within this design space. The RSM does not capture this effect. In fact the CFD implies that the mixing efficiency can actually improve when the injection angle is reduced, under certain conditions. For example, consider the comparison shown in Figure 10. The sole difference between the two cases was the transverse injection angle (75° versus 15°). The steeper injection clearly penetrates very early and establishes the bulk of fuel along the centerline. However, the mixing must then occur outward from the centerline. The shallower injection does not penetrate to the centerline, yet spreads towards this region from both

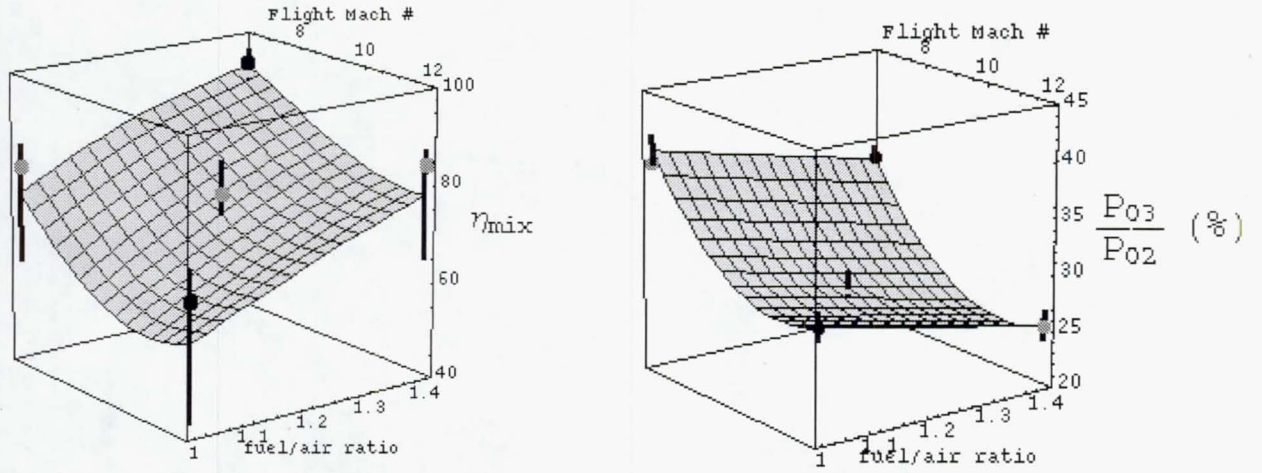

Figure 12 Performance map of the FWD-15° injector configuration: surrogate models are represented as the gray surfaces, the associated 95% confidence intervals are indicated by the vertical lines, test data shown as black dots, and confirmation data shown as gray dots.

above and below. Different 3D flow patterns emerge, along with different 1D mixing profiles. This effect was even more dramatic at the fuel-rich conditions, shown in Figure 11. This effect appeared to change with freestream Mach number: this implies at least a three-way interaction between variables. The original experiment design (½-CCD) cannot resolve these effects. Further augmentation of the design is required, and will serve to tighten the 95% confidence bounds about the response models. However, the forward-positioned, low-angle injector configuration (FWD-15°) looked promising and deserved further attention.

One primary goal of this initial analysis was the development of a performance map for mixing efficiency across the scramjet portion of trajectory. The carpet plot depicted in Figure 12 revealed the current level of performance associated with the FWD-15° configuration discussed above. Notice that the new CFD cases lie within the statistical error bars, which was encouraging. However, the 95% confidence interval was rather large, and the data consistently skewed to one side of the prediction. This should be interpreted to mean that further definition of the design space can be expected to improve the predictive capabilities of these results.

If the mesh-dependant error (~5%) dominates the statistical error, as expected, then final analysis with fine mesh resolution would be appropriate.

FUTURE PLANS

While the scramjet results presented above are very encouraging, the target combustion efficiency of 92.5% has not been validated to date with this CFD analysis for Mach numbers above 6.5. Furthermore, this target efficiency must be realized at different axial stations, upstream of station #3, as the Mach number increases from 6.5 to 12. Future efforts aimed at modeling the axial profile of mixing efficiency will enable this analysis. The uncertainties associated with the surrogate models of mixing efficiency and total pressure recovery are still too large to adequately capture the finer details of this complex design space. This is due, in part, to the fractional nature of the experimental design chosen. Additional calculations, which will complete a full central-composite experiment design, should significantly reduce the uncertainty associated with modeling. A design optimization should be postponed until these additional simulations are complete.

Another important feature of this injector design has yet to be fully examined. The initial study neglected to include transverse injector pitch as a design space variable. The pitch was fixed at six degrees for all cases. An examination of the flowfield contours that result from each calculation (not shown) revealed that the mixing results are very three-dimensional in nature. The best performances observed within this study exhibit excellent mixing in the transverse direction, while relatively less mixing in the circumferential direction. The dominant variable controlling the circumferential distribution of fuel is, of course, the pitch between injectors. Future efforts are aimed

at exploring these 3D features in order to achieve an optimal fueling scheme. The long-term goal is to take the quantitative trends derived with CFD and optimize the performance for a physical test article.

With regards to the Mode 1 analysis, simulation of the IRS cycle operation is currently underway. Comparison with the conventional ejector ramjet performance will be made. The eventual goal of this research program is use of the CFD analysis capability to examine time-dependent engine performance issues, such as:

1. Power-on of hydrogen fuel during initial stages (~Mach 1) of Mode 1 flight, initial formation and stabilization of thermal throat.
2. Modulation of thermal throat position through radial / axial fuel injection.
3. Flameholding effects during transition to Mode 2, accompanied by rapid loss of rocket power.

In all these situations, a short-term perturbation occurs which may have rapid, possibly destabilizing effects on the entire flowpath. A clear understanding of such transient effects and how (or if) engine stability is achieved after modulation is critical for constructing fuel scheduling maps and in predicting engine performance more precisely.

CONCLUSIONS

The present work has demonstrated a 3D analytical capability for subsonic combustion within a semi-annular flowpath. Two cold flow and one hot flow simulations have been conducted. The agreement with available data has been encouraging. The current results demonstrate the difficulty of relying upon the conventional ejector-ramjet cycle to effectively mix and burn excess fuel provided a fuel rich rocket alone. The length required for complete mixing was greater than the geometry examined. However, this analytical technique can be applied to investigate the combustion phenomenon of the independent-ramjet-stream cycle for the GTX propulsion system.

The present work also demonstrates an initial performance optimization capability for the supersonic combustion mode. Mixing efficiency and total pressure recovery results were reported for 27 separate 3D frozen-chemistry simulations. The output has been modeled and an initial high-performance injector geometry has been identified. However, the 3D complexity of this flowfield demands that further analysis (both CFD and statistical) is required to capture the important variable interactions between injector angle, location, freestream Mach number and total equivalence ratio. The target combustion efficiency level of 92.5% does appear to be a reasonable assumption for continued cycle analysis, although this has not been validated to date. Note that for the current injector design, this target efficiency becomes more elusive as the freestream Mach number approaches twelve.

REFERENCES

[1] Trefny, C. J. "An Airbreathing Launch Vehicle Concept for Single Stage to Orbit," AIAA 99-2730, 35th AIAA/ASME/SAE/ASEE Joint Propulsion Conference and Exhibit, June 20-23, 1999

[2] Steffen, C. J. Jr., and Yungster, S., "Computational Analysis of the Combustion processes in an Axisymmetric, RBCC Flowpath," NASA TM 2001-210679

[3] Yungster, S., and Trefny, C. J., "Analysis of a New Rocket-Based Combined-Cycle Engine Concept at Low Speed," AIAA 99-2393, , 35th AIAA/ASME/SAE/ASEE Joint Propulsion Conference and Exhibit, June 20-24, 1999.

[4] Walker, J. F., Kamhawi, H., Krivanek, T. M., Thomas, S. R., and Smith, T. D.; "Status of the RBCC Direct-Connect Mixer-Combustor Experiment," to be presented at JANNAF CS/APS/PSHS/MSS Joint Meeting – Apr. 8-12, 2002 Destin, FL

5 Roy, C.J. and Edwards, J.R. "Numerical Simulation of a Three-Dimensional Flame / Shock Wave Interaction," AIAA Journal, Vol. 38, No. 5, 2000, pp. 745-753.

[6] McDaniel, K.S. and Edwards, J.R. "Simulation of Thermal Choking in a Model Scramjet Combustor," AIAA Paper 99-3411, June, 1999.

[7] McDaniel, K.S. and Edwards, J.R. "Three Dimensional Simulation of Thermal Choking in a Model Scramjet Combustor", AIAA Paper 2001-0382, Jan. 2001

[8] Edwards, J.R. "A Low-Diffusion Flux-Splitting Scheme for Navier-Stokes Calculations," Computers & Fluids, Vol. 26, No. 6, 1997, pp. 635-659.

[9] Liou, M.-S. "A Sequel to AUSM: AUSM(+)," Journal of Computational Physics, Vol. 129, No. 2, 1996, pp. 364-382.

[10] Balakrishnan, G., Smooke, M.D., and Williams, F.A. "A Numerical Investigation of Extinction and Ignition Limits in Laminar Nonpremixed Counterflowing Hydrogen-Air Streams for Both Elementary and Reduced Chemistry," Combustion and Flame, Vol. 102, No. 3, 1995, pp. 329-340.

[11] McClinton, C. R., Ferlemann, S. M., Rock, K. E., and Ferlemann, P. G., "The role of formal experiment design in hypersonic flight system technology development," AIAA-2002-0543, Reno, NV, 2002

[12] McClinton, C. R., "Scramjet Combustor Design Methodology," First National Aerospace Plane Technology Symposium, NASA Langley Research Center, Hampton, VA, May 1986

[13] Hack, K. J., and Riehl, J. P., "Trajectory Development and Optimization of an RBCC-based Launch Vehicle," AAS 99-347, AAS/AIAA Astrodynamics Specialist Conference, Girdwood, AK, 16-19 August, 1999.

[14] Wilcox, D. C., Turbulence Modeling for CFD, second edition, DCW Industries, Inc, La Canada, CA, July, 1998 (see page 122 of the second printing for a description of the 1998 version of the k-ω model)

[15] Steffen, C. J., Jr., "Response Surface Modeling of Combined-Cycle Propulsion Components Using Computational Fluid Dynamics," AIAA 2002-0542, Reno, NV, 2002

[16] **CRC Standard Mathematical Tables**, 28th edition, W. H. Beyer, editor, CRC Press, Boca Raton, Florida, 1987.

[17] Paull, A. and Stalker, R. J., **Scramjet Propulsion**, *Volume 189 of the Progress in Aeronautics and Astronautics series*, Curran, E. T., and Murthy, S. N. B. editors; Zarchan, P., Editor-in-Chief; American Institute of Aeronautics and Astronautics, Inc., 2000; see chapter 1.

REPORT DOCUMENTATION PAGE

Form Approved
OMB No. 0704-0188

1. AGENCY USE ONLY (Leave blank)	2. REPORT DATE	3. REPORT TYPE AND DATES COVERED
	June 2002	Technical Memorandum

4. TITLE AND SUBTITLE

Three Dimensional CFD Analysis of the GTX Combustor

5. FUNDING NUMBERS

WU–708–90–63–00

6. AUTHOR(S)

C.J. Steffen, Jr., R.B. Bond, and J.R. Edwards

7. PERFORMING ORGANIZATION NAME(S) AND ADDRESS(ES)

National Aeronautics and Space Administration
John H. Glenn Research Center at Lewis Field
Cleveland, Ohio 44135–3191

8. PERFORMING ORGANIZATION REPORT NUMBER

E–13357

9. SPONSORING/MONITORING AGENCY NAME(S) AND ADDRESS(ES)

National Aeronautics and Space Administration
Washington, DC 20546–0001

10. SPONSORING/MONITORING AGENCY REPORT NUMBER

NASA TM—2002-211572

11. SUPPLEMENTARY NOTES

Prepared for the Combustion, Airbreathing Propulsion, Propulsion Systems Hazards, and Modelling and Simulation Subcommittees Joint Meeting sponsored by the Joint Army-Navy-NASA-Air Force, Destin, Florida, April 8–12, 2002. C.J. Steffen, Jr., NASA Glenn Research Center; R.B. Bond and J.R. Edwards, North Carolina State University, Raleigh, North Carolina 27695–7910. Responsible person, C.J. Steffen, Jr., organization code 5880, 216–433–8508.

12a. DISTRIBUTION/AVAILABILITY STATEMENT

Unclassified - Unlimited
Subject Category: 01 Distribution: Nonstandard

Available electronically at http://gltrs.grc.nasa.gov/GLTRS

This publication is available from the NASA Center for AeroSpace Information, 301–621–0390.

12b. DISTRIBUTION CODE

13. ABSTRACT ***(Maximum 200 words)***

The annular combustor geometry of a combined-cycle engine has been analyzed with three-dimensional computational fluid dynamics. Both subsonic combustion and supersonic combustion flowfields have been simulated. The subsonic combustion analysis was executed in conjunction with a direct-connect test rig. Two cold-flow and one hot-flow results are presented. The simulations compare favorably with the test data for the two cold flow calculations; the hot-flow data was not yet available. The hot-flow simulation indicates that the conventional ejector-ramjet cycle would not provide adequate mixing at the conditions tested. The supersonic combustion ramjet flowfield was simulated with frozen chemistry model. A five-parameter test matrix was specified, according to statistical design-of-experiments theory. Twenty-seven separate simulations were used to assemble surrogate models for combustor mixing efficiency and total pressure recovery. ScramJet injector design parameters (injector angle, location, and fuel split) as well as mission variables (total fuel massflow and freestream Mach number) were included in the analysis. A promising injector design has been identified that provides good mixing characteristics with low total pressure losses. The surrogate models can be used to develop performance maps of different injector designs. Several complex three-way variable interactions appear within the dataset that are not adequately resolved with the current statistical analysis.

14. SUBJECT TERMS	15. NUMBER OF PAGES
Computational fluid dynamics; Ramjet; Combustion	20
	16. PRICE CODE

17. SECURITY CLASSIFICATION OF REPORT	18. SECURITY CLASSIFICATION OF THIS PAGE	19. SECURITY CLASSIFICATION OF ABSTRACT	20. LIMITATION OF ABSTRACT
Unclassified	Unclassified	Unclassified	